

Adduct-specific monoclonal antibodies for the measurement of cisplatin-induced DNA lesions in individual cell nuclei

Bernd Liedert, Dick Pluim¹, Jan Schellens¹ and Jürgen Thomale*

Institut für Zellbiologie, Universitätsklinikum Essen, Germany and ¹Department of Experimental Therapy, The Netherlands Cancer Institute, Amsterdam, The Netherlands

Received January 19, 2006; Revised February 2, 2006; Accepted February 23, 2006

ABSTRACT

The anticancer drug cisplatin executes its cytotoxic activity via formation of intra- and interstrand crosslinks in DNA. The relative contribution of structurally defined cisplatin adducts to induce apoptosis and the cellular processing of these lesions is still poorly understood mostly due to the lack of sensitive analytical tools for *in vivo* studies. Here we describe a new method to establish and characterize monoclonal antibodies (Mab) for structurally defined DNA adducts. The two major reaction products of cisplatin, the guanine–guanine (Pt-[GG]) and adenine–guanine (Pt-[AG]) intrastrand crosslinks are recognized by Mab R-C18 and R-B3, respectively. Both antibodies were employed in an immuno-cytological assay allowing the quantification of drug-induced lesions in individual cell nuclei at clinically relevant doses. Analyzing various tissues of cisplatin-treated C57Bl/6 mice the accumulation of Pt-(GG) was highest in kidney tubular cells compared with 30, 50 and 90% lower levels in kidney stroma, liver and peripheral blood cells, respectively. Adduct kinetics revealed that wild type mouse cells remove up to 80% of the crosslinks in contrast to their complete persistence in nucleotide excision repair-deficient (XPC^{-/-}) mice. The aptitude of the immunoassay for human molecular dosimetry studies was demonstrated by measuring adduct levels in tumor biopsies from patients treated with cisplatin.

INTRODUCTION

The inorganic platinum (Pt) drug molecule cisplatin (*cis*-diamminedichloroplatinum [II]), first described as an antineoplastic agent in 1965 by Rosenberg *et al.* (1), is among the most

frequently used chemotherapeutics for the treatment of a broad range of solid tumors [reviewed in (2,3)]. The efficacy of platinum-based chemotherapy is hampered by two major obstacles, the development of cellular and clinical resistance [reviewed in (4,5)], leading to therapeutic failure and dose-limiting side effects like nephro- (6), neuro- (7) or ototoxicity (8).

Both, the antineoplastic activity and the dose-limiting toxicities of cisplatin result from the formation of reaction products with DNA in target cells. The intracellular exchange of chloro- to hydroxo-ligands in the molecule initiates a fast formation of DNA monoadducts preferentially at nucleophilic N-atoms of purines. This reaction is followed by a comparable slow conversion into bivalent intra- and interstrand crosslinks within hours [reviewed in (9)]. Four different structures, linked at the N-7 position of adenines and guanines, have been identified: the intrastrand adducts *cis*-Pt(NH₃)₂d(pGpG) (abbreviated as Pt-[GG]), *cis*-Pt(NH₃)₂d(pApG) (abbreviated as Pt-[AG]) and *cis*-Pt(NH₃)₂d(pGpXpG), representing >95% of total DNA platination and the interstrand lesion *cis*-Pt(NH₃)₂d(GMP)₂ (10,11). The degree of DNA adduct formation by cisplatin is cell type-specific (12) due to a number of pharmacokinetic parameters like kidney function (13), drug export by MRP2 membrane transporters (14) or cytoplasmatic detoxification (15). Some of these factors may also contribute to the observed inter-individual differences in the level of DNA platination after treatment with cisplatin. The removal of platinated DNA (Pt-DNA) intrastrand crosslinks has been linked to nucleotide excision repair (NER) (16,17) and to the NER sub pathway of transcription-coupled repair eliminating adducts from the transcribed strand of active gene sequences (18). Interstrand crosslinks are most likely processed by recombination repair mechanisms (19). The degree of tolerance to persisting (unrepaired) DNA lesions determines the fate of a given cell, which may be survival or apoptosis (2). The molecular mechanisms underlying resistance in the clinical setting might be decreased adduct formation, increased adduct repair or enhanced tolerance to cisplatin-induced

*To whom correspondence should be addressed. Tel: +49 201 723 4230; Fax: +49 201 723 5904, Email: juergen.thomale@uni-essen.de

lesions. Owing to the lack of sensitive analytical methods for a fast and reliable measurement of DNA platination products at the level of individual cells or in defined gene sequences, the relative contribution of the different mechanisms for intrinsic or acquired resistance is far away from being understood. Furthermore, even the relative importance of the various, structurally defined DNA adducts for both, the antineoplastic efficiency and the cell type specific toxicity, are still discussed controversially.

In order to improve the knowledge about the molecular mechanisms of cisplatin-related cytotoxicity, numerous analytical attempts have been made within the past 20 years to detect and measure Pt-DNA adducts in experimental systems and in clinical specimens. Among these methods are spectroscopic procedures like NMR (20), atomic absorption spectrometry (AAS) (21) or inductively coupled plasma mass spectrometry (ICP-MS) (22) as well as ^{32}P -postlabeling techniques (23–25). Further progress in understanding the molecular mechanisms which modulate the activity profile of cisplatin *in vivo* was hampered, because these methods are not sensitive enough to measure DNA platination at clinically relevant levels (NMR), or are unable to distinguish between specific lesions (AAS, ICP-MS), or do not permit single cell resolution (all methods).

Several attempts were made to quantify DNA platination products by immuno-analytical assays based on polyclonal or monoclonal antibodies (26–29). Two different strategies were applied to prepare antigens for this purpose. Fichtinger-Schepman *et al.* (20) immunized rabbits with isolated *cis*-Pt(NH₃)₂d(pGpG) or *cis*-Pt(NH₃)₂d(pApG) molecules. Antisera obtained thereby were capable to recognize the corresponding adducts in a competitive ELISA but only after a comprehensive nuclease digestion of isolated DNA followed by chromatographic isolation of the platinated dinucleotides. First attempt to detect cisplatin-induced DNA lesions at the single cell level by an immuno-histochemical assay were based on a polyclonal serum against Pt-DNA (12). Aiming at an adduct-specific measurement Tilby *et al.* (30), Chao *et al.* (31) and Sundquist *et al.* (32) independently generated monoclonal antibodies against cisplatin-treated DNA. Until now, however, most attempts failed to characterize these Mabs for their epitope specificity in genomic DNA. Recently, Meczes *et al.* (33) reported the binding of Mab CP9/19 to guanine–guanine intrastrand crosslinks. Here, we describe a new strategy to generate and characterize monoclonal antibodies with defined specificities for cisplatin-induced DNA adducts. Furthermore, we have used these Mabs to establish a quantitative immuno-cytological assay (ICA) which enables molecular dosimetry studies at the single cell level in experimental systems and in clinical samples.

MATERIALS AND METHODS

In vitro platination of DNA

For immunization of rats, development of ELISA, magneto-bead based separation of hybridomas and for the characterization of Mabs calf thymus DNA (Roche, Mannheim, Germany) was platinated according to Fichtinger-Schepman (20). A 1.6 mM stock solution of cisplatin in 150 mM NaCl (Platinex, Bristol, München, Germany) was diluted

with saline to final concentrations between 0.05 and 150 μM and incubated with DNA for 12 h at 37°C. The DNA preparations were purified by spin column centrifugation (BioSpin 6; BioRad, München, Germany) and the DNA concentration was quantified with the SYBR Green-I kit (Molecular Probes, Eugene). In collaboration with the Institut für Chemo- und Biosensorik (Münster, Germany) the molar content of platinum in DNA was determined according to Reed *et al.* (34) by AAS (Perkin-Elmer 4100 ZL; Perkin-Elmer, Norwalk).

Immunization

The antigen was synthesized according to Tilby *et al.* (30) by coupling cisplatin-treated DNA (Pt-DNA; 2100 $\mu\text{g}/\text{ml}$, 188 pmol Pt/ μg DNA) electrostatically to methyl-BSA [2100 $\mu\text{g}/\text{ml}$ in phosphate-buffered saline (PBS); Sigma, Deisenhofen, Germany]. BD IX rats (50 days old; Harlan-Winkelmann, Borcheln, Germany) were immunized by intraperitoneal injections of the Pt-DNA protein complex (530 μg containing 50 nmol adduct) dissolved in 250 μl MPL-TDM adjuvants (Sigma, Deisenhofen, Germany). Treatment was repeated every 4 weeks and the serum titer of the rats for anti-(Pt-DNA) antibodies was determined by ELISA measurement (see below) 10 days after injection. Immunized animals with a high titer were sacrificed 3 days after the last boost injection and hybridomas were established from spleen cells as described earlier (35).

ELISA

Antibody activity was determined by an ELISA procedure according to Sundquist *et al.* (32). Each well of a 96-well polystyrol microtiter-plate (Maxisorp, Nunc, Wiesbaden, Germany) was incubated with 200 μl DEAE dextran (100 $\mu\text{g}/\text{ml}$; Amersham Pharmacia, Freiburg, Germany) in 1 M Na₂CO₃, 5 mM EDTA, pH 9.6 for 5 h at 37°C. After washing with PBS wells were coated with untreated DNA or with Pt-DNA (188 pmol Pt/ μg), irradiated for cross-linking (0.12 J; UV Stratalinker 2400, Stratagene, La Jolla), and blocked with casein (1% in PBS; 1 h; 37°C; Schleicher & Schuell, Dassel, Germany). Per well 50 μl of diluted serum, hybridoma supernatant or chromatographic fractions, were incubated (1 h at 37°C). The antibody activity was detected by an alkaline phosphatase-labeled sheep anti-(rat Ig) antibody (50 $\mu\text{l}/\text{well}$; Dianova, Hamburg, Germany), using 1 mg p-nitrophenyl phosphate/ml (Sigma) in 10 mM diethanolamine, 1 mM MgCl₂, pH 9.8 as substrate. Absorption was measured at 405 nm (micro plate reader ELx 800; Bio-Tek Instruments, Neufahrn, Germany).

Magneto-bead based isolation of hybridomas

After cell fusion the heterogeneous pools of hybridomas were selected for cells presenting membrane-anchored anti-(Pt-DNA) antibodies by a magneto bead technique (36). Magneto beads (four times 108/ml; Type M 450, Dynal, Hamburg, Germany) were incubated in poly-L-lysine solution (50 $\mu\text{g}/\text{ml}$; Sigma) for 4 h at 37°C and then coated with Pt-DNA (1000 $\mu\text{g}/\text{ml}$; 5 pmol Pt/ μg ; incubation for 4 h at 37°C followed by 12 h at 4°C). Nonspecific binding was blocked with RPMI 1640 medium containing 20% fetal calf serum (FCS). Hybridoma cells (106) and beads (107) were mixed

in 1 ml of RPMI medium under constant agitation according to Ossendorp *et al.* (37) for 15 min at 25°C, followed by a 2 h incubation at 4°C. Bead-labeled cells were isolated via magnetic separation (MPC magnet, Dynal), washed twice with ice-cold medium, diluted to low concentrations and seeded into microtiter plates for further cultivation (38).

Cell culture of hybridomas and isotyping of Mabs

After hypoxanthine-aminopterin-thymidine (HAT)-selection hybridomas were cultivated in serum-free medium (Hybridoma-SFM; Invitrogen, Karlsruhe, Germany). Isotyping for immunoglobulin subclasses was performed by an ELISA technique according to Coulter *et al.*, (39) using isotype specific anti-(rat-Ig) antibodies (Sigma).

Purification of antibodies

Antibodies were isolated from hybridoma supernatant according to Hutchens and Porath (40) by hydrophobic interaction chromatography on T-gel (Pierce, Rockford, USA) and subsequent protein G column chromatography (HiTrap Protein G; Amersham Pharmacia, Freiburg, Germany). Antibody concentration was measured by a 'Capture ELISA' technique according to Fleming and Pen (41), antibody activity by the ELISA described above.

Adduct specificity of Mabs

The adduct-specificity of a given anti-(Pt-DNA) Mab was determined by measuring the relative adduct content in DNA fragments captured by this Mab in a filter binding assay. Briefly, calf thymus DNA was reacted with different concentrations of cisplatin (see above) resulting in fractions containing 0.52 (Pt 1), 1.01 (Pt 2) or 5.02 (Pt 3) pmol Pt/ μ g DNA. Fractions were adjusted to 50 mM Tris-HCl, 100 mM NaCl, 1 mM EDTA, pH 7.5 (STE buffer) and the DNA was fragmented by ultrasonic treatment (Sonifier B 12, Branson; five times 1 min on ice) to a medium length of 500 bp as determined by agarose gel electrophoresis. Aliquots of 50 μ g DNA in 60 μ l STE buffer containing 500 μ g BSA/ml were mixed with 100 μ g (in 40 μ l STE) of the monoclonal anti-(Pt-DNA) antibody to be characterized and incubated for 12 h at 4°C. Mab-complexed DNA was separated from unbound DNA fragments by soaking the solution through nitrocellulose filters (2 \times 2 cm; Protran BA 85, Schleicher & Schuell, Dassel, Germany). The captured DNA fragments were recovered from the Mab-DNA complexes by agitating the membranes in small volumes of elution buffer (5 mM Tris-HCl, 0.1 mM EDTA, 5% butanol, pH 7.5) for 48 h at 25°C. The eluate was concentrated, desalted by gel filtration (BioSpin 6, BioRad, München), and the DNA content was measured fluorimetrically (SYBR Green I kit; Molecular Probes, Leiden, ND).

Digestion of isolated DNA fragments, chromatographic separation of platinated dinucleotides, chemical deplatination, ³²P-postlabeling and high-performance liquid chromatography separation of labeled dinucleotides were performed essentially as described earlier (25) with some modifications: 50 μ g (in 50 μ l) of each Mab-selected DNA-fraction were digested by adding 6 U of nuclease P1 (Roche) and incubated for 2 h at 55°C. After conditioning with 10 μ l of 1 M Tris-HCl, 10 mM MgCl₂, 1 mM ZnCl₂, pH 8.2 digestion to nucleotides was continued by adding 100 U DNase (2 h at 37°C; Roche)

and subsequent treatment with 20 U alkaline phosphatase (2 h at 37°C; Roche). Enzymes were inactivated (100°C, 5 min) and removed by extraction with an equal volume of phenol/chloroform/isoamylethanol (25/24/1, v/v). Traces of phenol were removed by extraction with an equal volume of chloroform. The platinated dinucleotides were separated from the unmodified mononucleosides by strong cation-exchange chromatography using SCX solid phase extraction cartridges (Lichrolut SCX, 200 mg; Merck, Darmstadt, FRG) and a vacuum manifold. Cartridges were equilibrated with 1 ml of Tris-HCl (50 mM, pH 3) and the DNA digests were adjusted to pH 3 by HCl prior to loading. Non-adducted nucleosides were eluted by Na-formate (5 mM, pH 6; eight times 1 ml) followed by elution of the platinated products with NH₄OH (250 mM; 1 ml). This fraction was spiked with 300 fmol dTpdT (Sigma) as internal standard. Samples were dried *in vacuo*, the residues were dissolved in 12 μ l NaCN (100 mM) and incubated for 2 h at 65°C to deplatinate the Pt-dinucleotides. Then, samples were adjusted to pH 8 by addition of 7 μ l of 3 M Na-acetate solution. External standards were prepared from authentic dApdG and dGpdG dinucleotides (100 fmol each).

The 5'-³²P-postlabeling of dinucleotides was catalyzed by 2.5 U polynucleotide kinase (Roche), using 1.65 pmol [γ -³²P]ATP (3,000 Ci/mmol; 10 mCi/ml; Amersham Pharmacia). After overnight incubation at RT the volume was adjusted to 150 μ l with H₂O and the molar content of labeled dinucleotides was determined by radio-chromatography. Of each sample 50 μ l was applied on a heated Inertsil ODS-80A C-18 column (particle size: 5 μ m; dimension: 4.6 \times 150 mm; Phase Separations, Waddinxveen, ND) coupled to an on-line radioisotope detector (Radiomatic 500TR flow scintillation analyzer, Canberra Packard, Meriden). Products were separated by isocratic elution (100 mM KH₂PO₄/4.5% MeOH, pH 5.5; flow: 1 ml/min; 40°C) over a period of 16 min. Simultaneous Cerenkov radiation and absorption at 260 nm was measured every 6 s.

Immuno-cytological assay

Cells were cultured on microscopic slides, and washed with a starch solution (HAES-steril, Fresenius, Bad Homburg, Germany; 25% in PBS). Tissue sections and cell suspensions were placed onto pre-coated slides (ImmunoSelect, Squarix, Germany). All slides were air-dried and stored at -80°C until further processing.

The immunostaining of DNA adducts was performed essentially as described elsewhere (42) with some modifications. Briefly, samples were fixed in methanol (-20°C; 12 h) and rehydrated in PBS (10 min; 25°C). Each of the next steps was followed by washing with PBS. Cellular RNA was digested by RNase treatment (RNase A, 200 μ g/ml; RNase T1, 50 U/ml in PBS; 100 μ l per slide; Roche; 1 h; 37°C) in a humidified chamber. Nuclear DNA was partly denatured by mild treatment with alkali (70 mM NaOH, 140 mM NaCl, 40% methanol v/v; 5 min at 0°C), and cellular proteins were removed by a two-step proteolytic procedure: Samples were first digested with prewarmed pepsin (Roche; single cells, kidney and liver sections, 200 μ g/ml; gastric mucosa, 1000 μ g/ml in 20 mM HCl) for 5 min (cells) or 10 min (tissues) at 37°C, and then with prewarmed proteinase K (cells, 2 μ g/ml, tissues,

100 µg/ml in 20 mM Tris-HCl, 2 mM CaCl₂, pH 7.5; Merck) for 5 min (cells) or 10 min (tissue) at 37°C. After blocking with casein (1% in PBS; 30 min; 25°C) slides were incubated with anti-(Pt-DNA) Mabs (0.1 µg/ml in PBS containing 1% casein and 200 µg of sonicated calf thymus DNA/ml; 2 h; 37°C). After washing (0.05% Tween 20 in PBS; 2 min; 25°C) a three-step sandwich immunostaining was performed by subsequent incubation with: (i) FITC-labeled goat anti-(rat Ig) (Dianova, Hamburg, Germany; 6.5 µg/ml in PBS, 1% casein; 45 min; 37°C), (ii) ALEXA FLUOR 488-labeled rabbit anti-(FITC) (5 µg/ml in PBS, 1% casein; 45 min at 37°C; Molecular Probes) and (iii) ALEXA FLUOR 488 goat anti-(rabbit Ig) (5 µg/ml in PBS, 1% casein; 45 min, 37°C; Molecular Probes). Finally, the nuclear DNA was counterstained with DAPI (1 µg/ml in PBS; 30 min; 25°C; Serva, Heidelberg, Germany) and cells were covered with Vectashield densification compound (Vector Laboratories, Burlingame).

Image analysis

Visualization and measurement of antibody- and DNA-derived fluorescence was performed by a microscope-coupled digital image analysis system (fluorescent microscope Axioplan, lens Plan-Neofluar 40×/0.75; mercury lamp HBO 100 W; DAPI filter, excitation 365 nm, emission 397 nm; FITC/ALEXA 488 filter, excitation 450–490 nm, emission 515–565 nm, Zeiss, Göttingen, Germany; charge-coupled device camera C4880, Hamamatsu Photonics, Herrsching, Germany; ACAS 6.0 Cytometry Analysis System, ACAS II, Dunn, Asbach, Germany). The nuclear DNA of single cells was localized and measured by the DAPI-derived signals and those pixels were scanned in parallel for antibody-derived ALEXA fluorescence. Integrated ALEXA signals from each nucleus were corrected for the corresponding DNA content and computed for at least 100 cells per slide.

Cisplatin treatment of cultivated cells

Jurkat cells (human T cell leukemia line; TIB-152; ATCC, Rockville) were cultivated in RPMI 1640 medium supplemented with FCS (10%), L-glutamine (2 mM) and penicillin (100 µg/ml) in a humidified atmosphere (5% CO₂, 37°C). Exponentially growing cells were exposed to various concentrations of cisplatin (0.5–10 µg/ml) for 2 h at 37°C. After washing, cells were transferred to fresh medium, further incubated for 1 h at 37°C, spun down and resuspended in PBS containing 25% starch solution (see above). Cells were placed on precoated microscopic slides and analyzed by ICA measurement (see above).

Cisplatin treatment of mice

Formation and repair of Pt-DNA adducts *in vivo* was measured in tissues or cells from male C57Bl/6 mice (age, 20 weeks; Harlan-Winkelmann, Borchon, Germany) treated with a single intraperitoneal dose of cisplatin (Platinex, Bristol; 2 or 10 mg/kg body weight; untreated controls: sterile saline). XPC knockout mice were kindly provided by Dr Leon Mullenders, University of Leiden, ND. Animals were sacrificed at various time points after application by CO₂. Tissue samples were shock frozen in liquid nitrogen and cryo-sections (8 µm) were prepared using a Frigocut 2800 (Reichert-Jung, Nußloch, Germany). T lymphocytes were isolated from heparinized

peripheral blood (250 µl) by magneto beads coated with mouse pan T (Thy 1.2) antibodies (Dynal) according to the manufacturer's protocol. Beads were detached from isolated cells by trypsinization (15 min; 37°C; inactivation with FCS) and removed magnetically. Bead-free T cells were applied to microscopic slides as described above.

Human lymphocytes and bioptic material

Blood samples and bioptic specimens were kindly provided by Drs U. Vanhoefer and W. Eberhardt, Department of Internal Medicine (Cancer Research) West German Cancer Center Essen. Samples were taken from patients with gastric cancer before or after monotherapy with cisplatin (infusion time 1 h; Platinex, Bristol). T cells were isolated from heparinized peripheral blood (500 µl) by immuno-magnetic separation using anti-(CD2) coated beads (CD2 collection kit, Dynal) according to the manufacturer's protocol and bead-free T cells were applied to microscopic slides (see above). Biopsies of the primary tumor and of non-malignant adherent tissue were obtained endoscopically 48 h after administration of cisplatin and were frozen immediately in liquid nitrogen. Cryo-sections (8 µm) were prepared and mounted on slides (see above). Serial sections were alternatively immuno-stained for DNA adducts (ICA) or by Haematoxylin-Eosin (HE).

Data analysis

In all mouse experiments two treated and one control animal were used per time point and 50 sections were prepared from each organ. Per tissue sample 10 sections were chosen at random and analyzed by ICA. In total a minimum of 100 cells of each cell type per animal were analyzed. 'Sigma-Plot 4.0' software (Jandel Scientific, Erkrath, Germany) was used to calculate Pt-DNA adduct levels from integrated image signals. The results are given in relative units (mean ± SD or SE).

RESULTS AND DISCUSSION

Experimental design

In case of cisplatin-induced DNA lesions the two 'classical' methods to establish adduct-specific antibodies for immuno-histochemical detection of DNA damage have failed (see above). This indicates that the stereochemical motif recognized by antibodies against cisplatin adducts is completely different in small di- or oligonucleotide molecules in comparison with long chain genomic DNA.

Therefore, we have approached the generation of adduct-specific Mabs for single cell analysis by an alternative strategy comprising four major steps: (i) immunization of rats with highly adducted genomic DNA to provoke a broad immune response; (ii) selection for hybridoma clones producing Mabs with high binding affinity to low adducted DNA; (iii) 'retrospective' characterization of the binding specificity of individual Mabs by immuno-trapping of DNA fragments carrying recognized adducts, followed (iv) by the chromatographic identification of the trapped Pt-lesion(s). Finally, Mab clones with defined specificity were screened for their applicability in a quantitative ICA.

Table 1. Properties of cisplatin-reacted calf thymus DNA used for the characterization of anti-(Pt-DNA) monoclonal antibodies

DNA preparation	Pt 1	Pt 2	Pt 3
Cisplatin exposure (μM)	0.15	0.30	1.50
Platinum in DNA ($\text{pmol}/\mu\text{g}$) ^a	0.52	1.01	5.22
Nucleotides/Pt adduct	6250	3333	625
Adducts/500 bp fragment ^b	0.16	0.30	1.60
% of all 500 bp fragments carrying cisplatin adducts ^c	17	25	80
% of all adducted 500 bp fragments carrying			
1 adduct	92	86	41
2 adducts	7	12	32
3 adducts	1	3	17
4 adducts	0	1	6
5 adducts	0	0	3
6 adducts	0	0	2

^aAs determined by AAS measurement.^bAssuming a random distribution of adducts in DNA.^cCalculated according to a Poisson distribution.

Generation of monoclonal antibodies

For the generation and the characterization of suitable Mabs calf thymus DNA was reacted with different concentrations of cisplatin and the absolute content of platinum in the samples was determined by AAS (Table 1). To achieve a sufficient immune response against cisplatin adducts it is necessary to vaccinate rodents with highly Pt-DNA (27). The optimal adduct concentration for this purpose was determined to be 1 per 5 nt for mice (31) and 1 per 125 nt for rats (30). In this study we have immunized BD IX rats with cisplatin-reacted DNA (1 adduct/16 nt) coupled to methyl-BSA. Serum titers of anti-(Pt-DNA) antibodies were determined by a non-competitive ELISA using Pt-DNA as binding substrate.

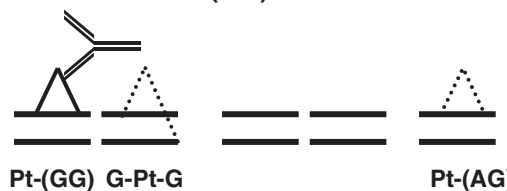
After a cumulative dose of 350 nmol Pt adducts per animal spleen plasma cells were fused with 'Y123' rat myeloma cells. To enrich the resulting hybridoma populations for antibodies which can recognize Pt adducts at low frequencies in DNA we used an immuno-magnetic separation technique (37,43). This method applying magneto beads coated with low-adducted DNA ('Pt-1'; 1 adduct/640 nt, see Table 1) selects for cell clones producing high affinity antibodies due to their stronger binding to the beads (44,45) and excludes Mabs which recognize stereochemical artifacts in highly adducted DNA. In comparison with the original hybridoma pool this pre-selection step led to a tenfold increase in ELISA-positive clones.

Adduct specificity of anti-(Pt-DNA) Mabs

As cisplatin-reacted DNA harbors a variety of distinct adduct structures (see above) in different sequence neighborhoods the heterogeneity of a Pt-DNA antigen provokes an immune response encompassing antibodies of different specificity. To characterize the binding motif of a given Mab clone we have designed a new experimental approach to determine the epitope specificity of monoclonal antibodies directed against structural modifications in genomic DNA (Figure 1). The basic idea of this method is to pull out from a large pool of DNA molecules just the fraction containing the modification(s)

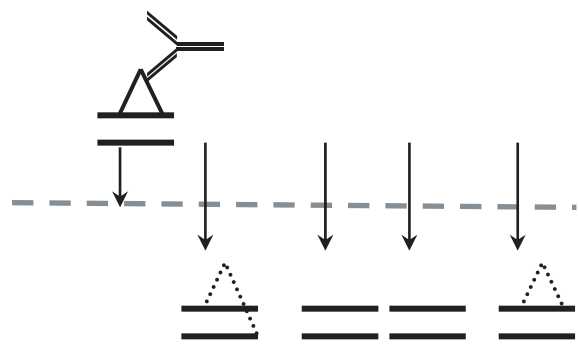
- Pt-DNA
 - ultrasonic fragmentation (~500 bp)
 - incubation with Mab

anti-Pt-(GG) Mab

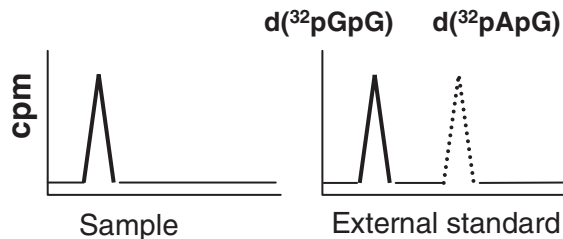


Pt-(GG) G-Pt-G Pt-(AG)

- binding of Pt-DNA Mab complexes on nitrocellulose
 - elution of unbound Pt-DNA



- detachment of Mab-trapped fragments
 - enzymatic digestion of Pt-DNA to nucleotides
dN, Pt-d(GpG)
 - cation-exchange chromatography → **dN**
Pt-d(GpG)
 - deplatination of Pt-dinucleosides
 - 5'- [³²P] labeling of dinucleotides
d(³²pGpG)
 - HPLC / radioisotope detector

**Figure 1.** Schematic diagram of immuno-trapping and ³²P-postlabeling procedures to determine the binding specificity of anti-(Pt-DNA) monoclonal antibodies.

which are recognized by the antibody. A prerequisite for such an immuno-trapping strategy is a sufficiently low adducted DNA substrate carrying as mean less than one lesion per molecule.

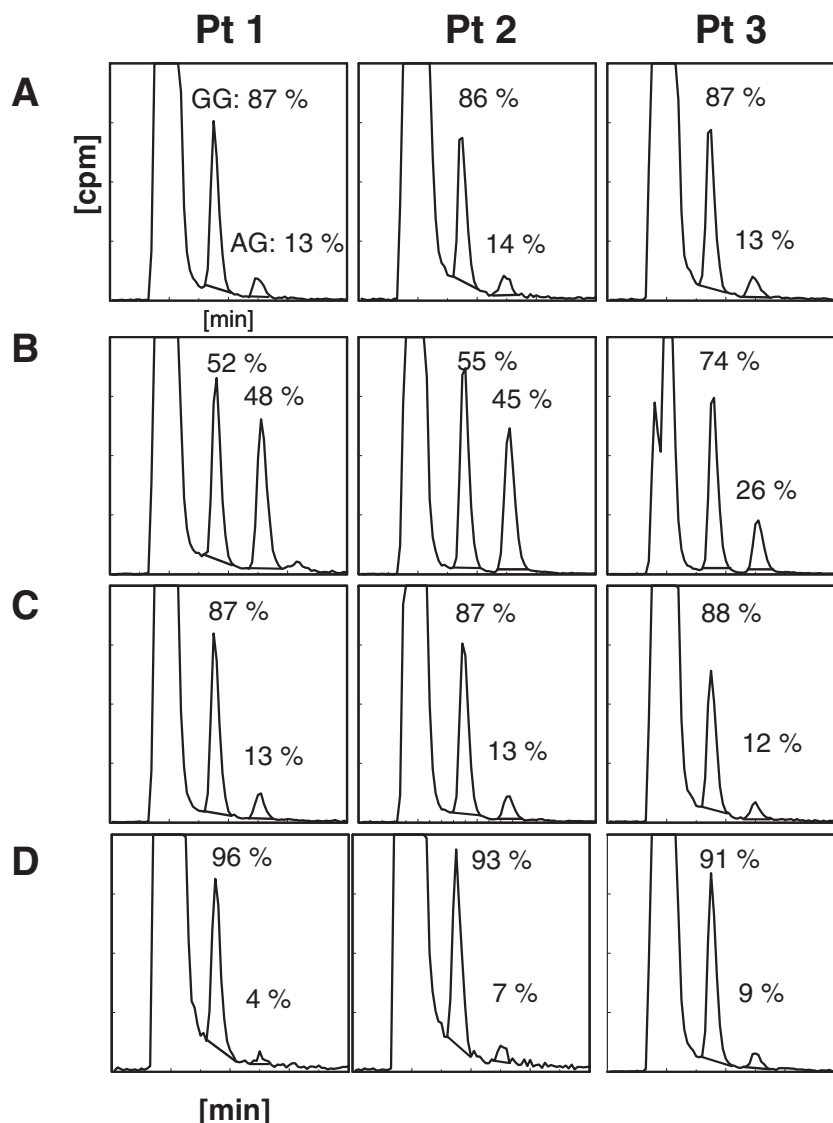


Figure 2. Radio-chromatographic analysis of the relative amounts of Pt-(GG) and Pt-(AG) intrastrand crosslinks in DNA preparations Pt 1–3 without antibody selection (A) or after the immuno-trapping procedure with Mab R-B3 (B), Mab R-C7 (C) or Mab R-C18 (D). The y-axes represent the ^{32}P -derived radioactive signals (c.p.m.), the x-axes give the elution time (min).

For this purpose double-stranded DNA fragments with an average size of 500 bp were prepared by ultrasonic treatment of Pt-DNA preparations ‘Pt 1’, ‘Pt 2’ and ‘Pt 3’ (Table 1). Assuming a random distribution of platination products, the mean number of Pt adducts per DNA molecule was calculated to be 0.16 (Pt 1), 0.3 (Pt 2) and 1.6 (Pt 3), respectively. According to the Poisson distribution, the percentage of adducted fragments carrying just one lesion was 92, 86 and 41% in the respective samples.

When these DNA substrates were incubated with antibodies to be characterized and passed through nitrocellulose membranes, only protein (Mab)-complexed double-stranded DNA molecules were retained. Filter-bound DNA fragments harboring the selected epitope(s) were then recovered from the membranes (Materials and Methods). As shown earlier, both separation steps, binding and elution of adducted DNA fragments, can be performed in a quantitative manner with efficiencies of >90% (46).

To identify the Mab-trapped modifications we have analyzed the eluted DNA fractions by a ^{32}P -postlabeling assay (25). When the DNA was digested enzymatically to mononucleosides Pt-GG and Pt-AG dinucleotides remained uncleaved and could be isolated chromatographically. After chemical deplatination and ^{32}P -postlabeling the dinucleotides were measured by radiochromatography. The identity of radioactive peaks was confirmed by co-application of authentic GG and AG dinucleotides in the procedure. Thereby, it was possible to determine the relative concentrations of Pt-(GG) and Pt-(AG) residues in the immuno-trapped DNA samples.

Adduct analysis of the unselected DNA substrates ‘Pt 1’, ‘Pt 2’ and ‘Pt 3’ exhibited relative contents of Pt-(AG) and Pt-(GG) of about 13–14% and 86–87%, respectively, independently from the original degree of platination (Figure 2A). This finding is in good agreement with data in the literature (20) and underlines the reproducibility and validity of the analytical procedure.

Using the antibody selection step we could show a strong binding preference of Mab 'R-B3' for Pt-(AG) adducts in DNA (Figure 2B). In substrate 'Pt 1', containing the lowest adduct level, the relative amount of Pt-(AG) was increased by immuno-trapping from 13% in unselected DNA to nearly 50%. Taking into account that 8% of the 'Pt 1'-fragments carried more than one lesion (most likely additional GG-adducts, see below and Table 1) and assuming a linear influence of the antibody binding during the selection step it can be estimated that Mab 'R-B3' has an at least four-fold higher affinity to Pt-(AG) as compared with Pt-(GG) in genomic DNA. The enrichment effect for the AG dinucleotides was less pronounced in the higher adducted substrates 'Pt 2' and 'Pt 3' (45 and 26% of AG, respectively). This observation can be attributed to the co-isolation of the 6.5 times more frequent Pt-(GG) lesion occasionally located on the same DNA molecule as 16% (Pt 2) and 60% (Pt 3) of those substrate molecules carried more than one adduct (Table 1).

A second Mab, 'R-C7' (Figure 2C) did not discriminate between Pt-(GG) and Pt-(AG) intrastrand lesions despite of its high affinity to cisplatin-reacted DNA as measured in ELISA and filter binding assays. The relative adduct distribution (13% AG; 87% GG) in the antibody-trapped DNA fractions was exactly the same as in the unselected substrate, independently from the initial degree of platination. This might indicate that both major interstrand cross-links share a common structural motif in genomic DNA which is recognized by 'R-C7'. Thus this antibody is a useful tool for the simultaneous detection of both cisplatin adducts.

Finally, Mab 'R-C18' was found to enrich the proportion of Pt-(GG) lesions by immuno-trapping to 96% in substrate 'Pt 1', to 93% in 'Pt 2' and to 91% in 'Pt 3' (Figure 2D). Indicating a high specificity of this antibody for the major DNA adduct. In this case the 'leveling effect' caused by fragments harboring more than one lesion in higher Pt-DNA was less pronounced. For statistical reasons the identity of co-isolated epitopes on the same fragment is most likely also Pt-(GG).

Taking together the results demonstrate the potency of our new method to determine the epitope-specificity of monoclonal antibodies raised against complex hapten structures in genomic DNA. In addition, the immune response in this approach is not restricted to adducts in a given sequence context as in synthetic oligonucleotide haptens and the hybridoma enrichment step selects for high affinity antibodies with a broad spectrum of binding characteristics.

Further characterization of the newly established Mabs confirmed earlier observations (29) that antibodies binding to cisplatin-induced adducts in native long chain DNA often have no affinity to these lesions in comparatively small molecules. When the Mabs were tested in a competitive ELISA synthetic 32mer single or double-stranded oligonucleotides harboring site specific Pt-(GG) or Pt-(AG) lesions showed no inhibitory effects (data not shown). This situation seems to be different for the monoclonal antibody CP9/19 which was recently characterized to be specific for Pt-(GG) adducts (33).

ICA for the visualization and measurement of cisplatin induced DNA adducts in the nuclei of individual cells

Mabs characterized for their binding specificity were further selected for the applicability in the ICA technique (42) which allows the quantification of DNA adducts at the single cell level. Nonspecific antibody binding was minimized by subjecting cells or tissue sections on microscopic slides to proteolytic treatment prior to the immunostaining. Cell loss during this step was avoided by using pre-coated adhesion slides (see above).

The sensitivity of the ICA procedure was further augmented by a multi-step 'sandwich' staining using FITC- and ALEXA 488-labeled secondary antibodies, followed by counterstaining with DAPI for nuclear DNA. Position, area and intensities of signals from individual cell nuclei were visualized by fluorescence microscopy and recorded by an image analysis system. Antibody-derived signals were normalized for the actual DNA content of a given cell and expressed as arbitrary fluorescence units (AFU).

The complete penetration of the antibodies and the homogeneous immuno-staining of the nuclear DNA by the ICA procedure were verified by tomography and 3D laser-scanning microscopy of cisplatin-treated cells (data not shown).

The sensitivity and the range of linearity of the ICA procedure were examined in a dose response experiment using the Mabs R-C18 [specific for Pt-(GG)] or R-C3 [specific for Pt-(AG)] to analyze cisplatin-exposed cultured human Jurkat T cells. The quantitative evaluation of fluorescence signals from DNA and antibody staining revealed a nearly linear correlation ($r^2 = 0.94$ and $r^2 = 0.90$) between drug concentration and the corresponding apparent levels of Pt-(GG) and Pt-(AG) DNA adducts, respectively (Figure 3). Both intra-strand crosslinks could be quantified by ICA analysis in the nuclear DNA of Jurkat cells exposed to cisplatin concentrations as low as 0.5 $\mu\text{g/ml}$.

Formation and processing of Pt-(GG) adducts in different cell types of cisplatin-treated mice

Techniques which depict DNA lesions at the level of individual nuclei are particularly important for the analysis of tissue sections as they are usually composed of different cell types. Therefore we have adapted the ICA technique to measure formation and repair kinetics of Pt-(GG) DNA adducts in cryo-sections from tissues of C57Bl/6 mice sacrificed at different time points after cisplatin treatment. As severe nephrotoxicity is one of the dose limiting side effects of cisplatin (6,47) we have immuno-stained kidney cells of exposed and untreated mice (Figure 4A). In comparison to very low background signals in the control tissue the ICA images showed that the nuclear DNA of all renal cells was highly adducted 24 h after drug application with distinct intercellular variations. The epithelial cells of kidney tubuli (tubuli recti proximalis) displayed a much brighter immuno-fluorescence staining than all other cell types of this tissue. The ACAS image analysis system used here allowed the differential measurement of selected cell nuclei within a given tissue section demonstrating the analytical power of the single cell measurement: (Figure 4B). The

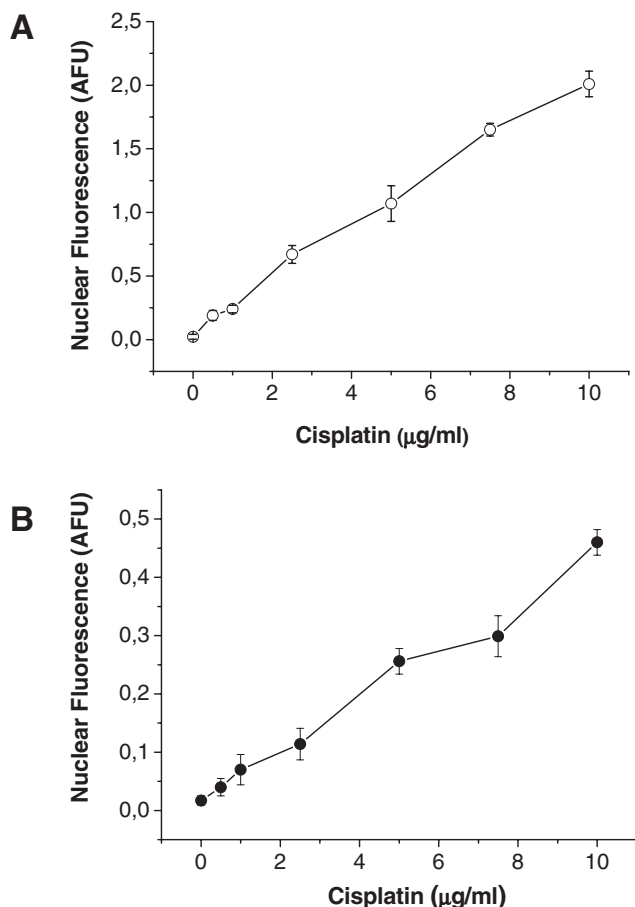


Figure 3. Correlation between the dose of cisplatin (exposure: 2 h; 37°C) and the level of specific intrastrand crosslinks in the nuclear DNA of cultivated human Jurkat T cells. Adduct levels were measured after immunostaining with anti-(Pt-DNA) Mab R-C18 (Pt-[GG] lesions (A), or R-B3 specific for Pt-[AG] (B) and quantitative ICA image analysis (Materials and Methods). Antibody-derived signals from individual nuclei were normalized for the actual DNA content of each cell. Values are given as AFU and represent means \pm SE of 200 analyzed cells per dose. Correlation: (A) $r^2 = 0.96$; (B) $r^2 = 0.91$.

quantitative evaluation of immuno-stained kidney sections revealed 50% higher adduct levels in the tubular cells when compared with the surrounding cortex cells (1.45 versus 0.95 AFU 24 h after cisplatin; $P < 0.05$, paired *t*-test; Figure 5). The relative differences between these two cell types were even more pronounced in mice sacrificed 2 weeks after cisplatin exposure (Figure 4A). At this time cortex and distal tubular cells had eliminated the majority of the initially formed Pt-(GG) adducts whereas the nuclear DNA of proximal tubuli epithelia still contained a burden of lesions comparable to the maximum adduct level in cortex cells at day one after treatment. The high degree of DNA platination in the tubular cells is most likely caused by the augmented intratubular concentration of free cisplatin during renal clearance in combination with a slightly acidic environment within the tubules, favoring the formation of reactive drug intermediates (48).

Quantitative ICA measurement of tissue sections and blood lymphocytes from cisplatin-treated mice revealed a broad range of peak adduct levels in different cell types

(Figure 5). Compared with tubular epithelial and cortex cells of the kidney where Pt-(GG) adducts reached a maximum of 1.82 and 1.15 AFU, respectively, the cells in liver sections exhibited a rather homogeneous immunostaining with a peak value of 0.80 AFU 12 h after treatment. In contrast, cisplatin-induced DNA damage in peripheral T lymphocytes of the same mice was about six and three times lower than in kidney tubular epithelia and in liver cells, respectively. Pt-(GG) adduct levels culminated at 0.25 AFU 8 h after drug application. Similar observations of a comparatively low DNA platination in white blood cells after cisplatin exposure *in vivo* or *in vitro* have been made earlier (49). Whether this is caused by pharmacokinetic factors like reduced influx, accelerated export or intracellular modification of the drug or by a more efficient repair of DNA platination products in T lymphocytes remains open.

To calibrate the relative adduct values based on ICA measurement for the absolute number of cisplatin-induced lesions per cell nucleus we have determined by AAS the molar content of platinum in DNA isolated from the same mouse tissue. Assuming that Pt-(GG) accounts for about 75% of the total DNA platination the peak formation level of this adduct after a dose of 10 mg cisplatin/kg body weight was calculated to be $\sim 800\,000$, $600\,000$ and $200\,000$ per cell in mouse kidney, liver and T lymphocytes, respectively. The lowest adduct level reproducibly measured was in mouse lymphocytes 2 weeks after drug treatment, corresponding to 25 000 Pt-(GG) lesions per nucleus.

Peak adduct levels were reached between 8 and 12 h after cisplatin application in all cell types analyzed here. This rather delayed accumulation of DNA crosslinks *in vivo* is probably due to a stepwise mobilization of the drug from plasma protein binding (50) and to the slow conversion of initially formed monoadducts to the bivalent crosslinks detected by the ICA measurement (51). The shapes of the Pt-(GG) repair kinetics were basically similar in all four cell types. After a period of fast repair where about 50–70% of the initially formed lesions were removed within 2–6 days the adduct levels reached a nearly stable plateau. Until day 15 only a minor fraction of the remaining Pt-(GG) lesions was removed in addition (Figure 5). Whether the persisting adducts at this time were less accessible for the cellular DNA repair system e.g. owing to their sequence context remains to be elucidated.

To further demonstrate the analytical power of adduct-specific ICA measurement we have compared the formation and repair of the Pt-(GG) lesion in specific cell types of mice proficient or deficient for NER. Kidney tubular epithelium cells of NER knockout (XPC^{-/-}) mice exposed to a low dose of cisplatin (2 mg/kg body weight) exhibited higher accumulation and complete persistence of this adduct in comparison to corresponding wild type cells with intact global genomic NER (Figure 6). Thus, the newly established immunoassay now allows the systematic *in vivo* analysis of adduct processing and drug-induced cytotoxicity in specific cells of transgenic or knockout mouse strains.

ICA measurement of Pt-DNA adducts as a tool for single cell dosimetry in clinical samples

Finally we have tested, whether the ICA procedure is sensitive enough to measure defined adducts in clinical specimens.

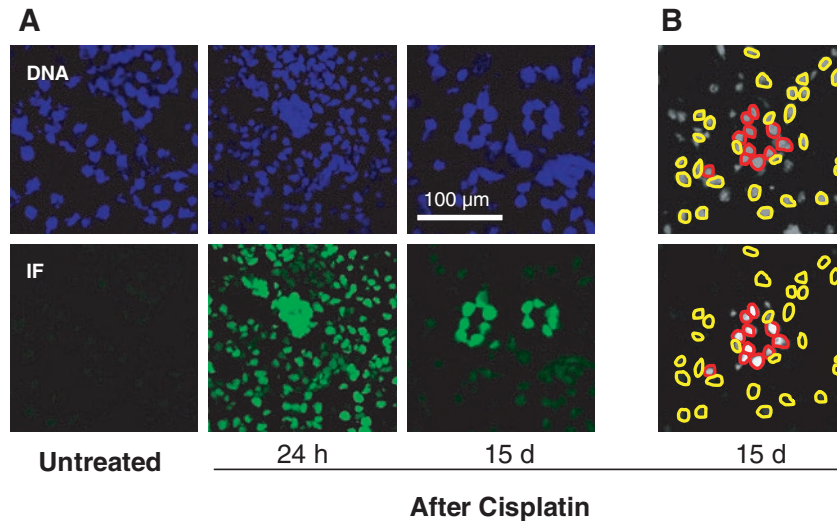


Figure 4. Visualization of Pt-(GG) intrastrand adducts in the DNA of individual mouse kidney cells by immunostaining. Male C57Bl/6 mice received a single injection of cisplatin (10 mg/kg intraperitoneal; untreated controls, 150 mM NaCl) and were sacrificed 24 h or 15 days later. Cryo-sections of kidney tissue were stained for DNA with DAPI (blue) and for Pt-(GG) in DNA by sandwich-immunostaining using Mab R-C18 (green; see Materials and Methods). (A) Micrographs of DNA and immuno-fluorescence (IF) on tissue sections from untreated or treated animals, (B) ICA image analysis of fluorescence-stained kidney cells (15 days after cisplatin). Cell nuclei were localized by DNA-DAPI signals and co-localized antibody-derived signals were recorded by the ACAS image analysis system. Specific cell types (e.g. tubulus epithelial cells marked in red) can be evaluated separately.

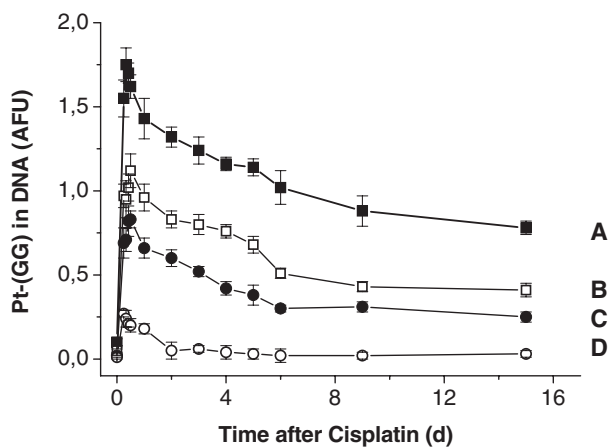


Figure 5. Formation and repair of Pt-(GG) intrastrand DNA adducts in different cell types of mice after cisplatin exposure. Male C57Bl/6 mice (age 20 weeks) were sacrificed before (t_0) or at various time points after a single injection of cisplatin (10 mg/kg, intraperitoneal; two animals per time point) and tissues were stored in liquid nitrogen. Blood T lymphocytes and frozen tissue sections (8 μ m) were prepared as described and Pt-(GG) adduct levels were measured by ICA analysis using Mab R-C18 (Figures 3 and 4). Values are means (\pm SE) of 200 measured cells per time point: A, kidney, epithelial cells of tubules proximalis; B, kidney cortex cells without tubules proximalis; C, liver cells; D, peripheral T lymphocytes. For a given time point adduct levels were significantly different (paired t -test: $P < 0.05$) between cell/tissue types A–D except for the comparison of B and C between days 5 and 15.

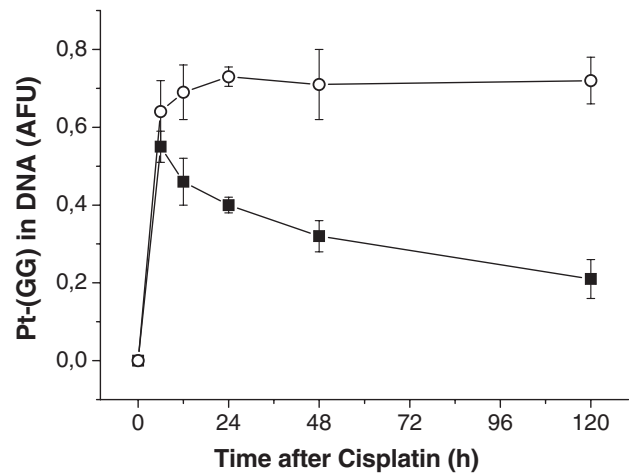


Figure 6. High accumulation and complete persistence of Pt-(GG) adducts in the DNA of kidney tubular epithelium cells of mice deficient for NER (XPC^{-/-}). XPC^{+/+} (wild-type, closed squares) and XPC^{-/-} mice (open circles) were treated with a single dose of cisplatin (2 mg/kg body weight, intraperitoneal) and kidney tissue sections were analyzed for DNA adduct levels as in Figure 5. Adduct levels were significantly different (paired t -test: $P < 0.05$) between both strains for time points >12 h.

Biopsies from three patients with advanced gastric cancer who had received a single infusion of cisplatin (30 or 50 mg/m²) were included in this pilot experiment. Samples from tumor areas and from adjacent normal tissue were taken before and 48 h after cisplatin infusion. Serial sections of post-treatment normal gastric mucosa stained either for histological examination with HE or for ICA analysis with DAPI and Mab

R-C18, demonstrated the applicability of this procedure (Figure 7A). Similar to the mouse experiments a very high adduct-specific staining was observed in post-treatment biopsies when compared with control biopsies prior to treatment (Figure 7B). Furthermore, higher magnification revealed distinct intercellular heterogeneities of DNA adduct levels within the same tissue section which may result from cell type specific formation and repair rates for Pt-(GG) adducts *in vivo*. This observation again underlines the importance of single cell analysis especially in clinical specimens and the necessity to

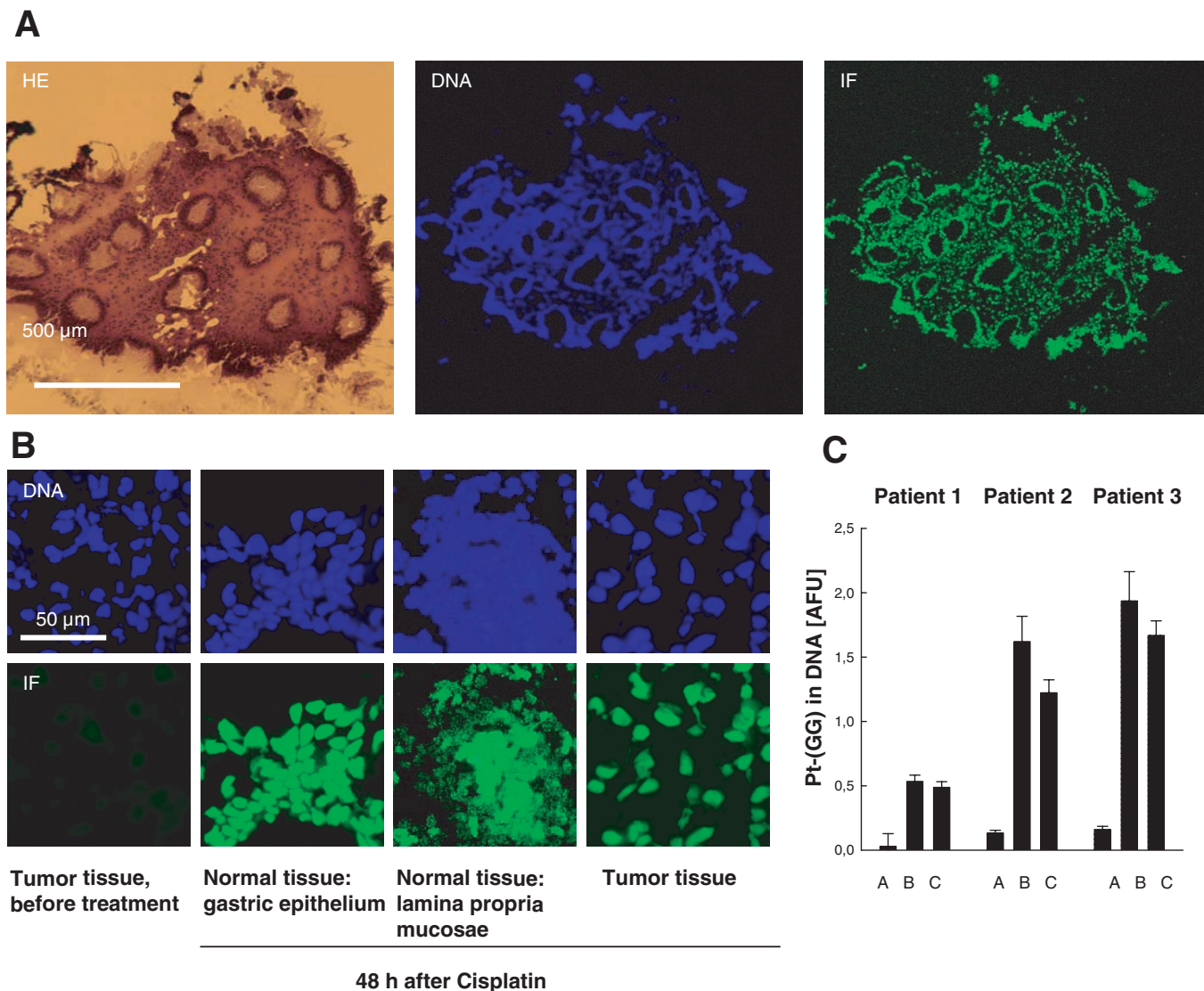


Figure 7. (A) Visualization of cisplatin-induced adducts in the nuclear DNA of stomach tissue cells from a patient treated for gastric cancer. Biopsies were taken 48 h after infusion of cisplatin (50 mg/m^2) and serial cryo-sections were alternatively stained with HE for morphology or by the ICA procedure for nuclear DNA (DAPI) and Pt-(GG) adducts (IF) using Mab R-C18. (B) Micrographs of ICA-stained cryo-sections of gastric tissue obtained before or 48 h after cisplatin treatment. Biopsies were taken both from the tumor and from adjacent normal tissue. DNA, DAPI-staining; IF, Pt-(GG)-specific immunostaining. (C) ICA-measurement of Pt-(GG) adduct levels in cell nuclei of gastric tissue from three patients treated with a single dose of cisplatin (patient 1, 30 mg/m^2 ; patients 2 and 3, 50 mg/m^2). A, biopsy before treatment; B, normal tissue 48 h after infusion; C, tumor cells 48 h after infusion. Columns represent mean values (\pm SE) of 100 cells selected at random.

define 'lead cell types' for molecular dosimetry studies. The quantitative evaluation of the immunostained biopsies indicated a dose dependency of adduct levels 48 h after treatment (Figure 7C). The mean Pt-(GG) values in tissue sections from patient 1 who received $30 \text{ mg cisplatin/m}^2$ were significantly lower both in the tumor and in adjacent normal gastric mucosa than the adduct burden in biopsies from patients 2 and 3 (50 mg/m^2).

To compare adduct levels in tumor site biopsies and in easily accessible cells of the same individual we have isolated normal T lymphocytes from the peripheral blood of patients at different time points after treatment. ICA analysis of Pt-(GG) levels revealed very homogeneous antibody-derived signals within a given cell sample

(Figure 8) and steadily increasing adduct levels between 1 and 48 h after cisplatin-infusion (data not shown) indicating that in this patient the ongoing formation of Pt-(GG) crosslinks is still dominating the efficiency of DNA repair processes. Similarly to our findings in mice, the rate of adduct formation in peripheral T lymphocytes of patients was markedly lower than in other cell types e.g. of the gastric mucosa. Again, the underlying pharmacokinetic and/or biochemical mechanisms are still unknown. Owing to the small number of patients included in this study it could not be decided yet whether the measurement of specific DNA platination products in blood-derived cells can serve as a surrogate marker for the adduct burden of tumor cells as has been suggested earlier (26,52).

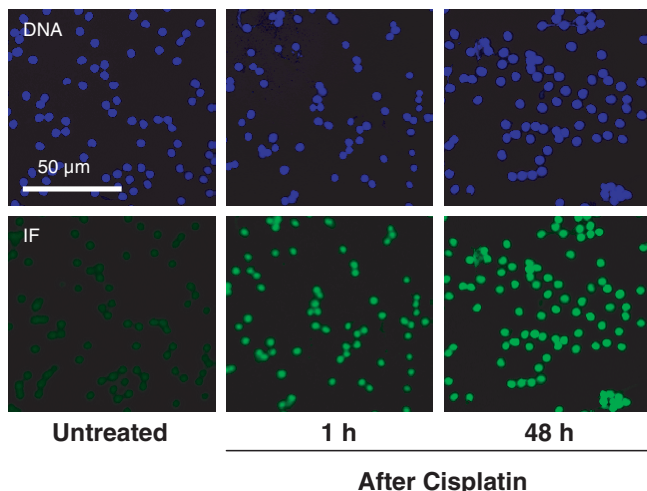


Figure 8. Immunostaining of Pt-(GG) DNA adducts in T lymphocytes isolated from the peripheral blood of patient 2 before and 1 or 48 h after cisplatin infusion (50 mg/m²; Figure 7).

ACKNOWLEDGEMENTS

We thank Drs Udo Vanhoefer and Wilfried Eberhardt [Department of Internal Medicine (Cancer Research), University of Essen] for providing tumor biopsies, the lab of Dr Leon Mullenders (University of Leiden, ND) for the generous gift of XPC knockout mice and Beate Karow for expert technical assistance. This work was supported by Deutsche Forschungsgemeinschaft Grant FOR 236/TP1B to J.T. Funding to pay the Open Access publication charges for this article was provided by Institut für Zellbiologie, Universitätsklinikum Essen.

Conflict of interest statement. None declared.

REFERENCES

- Rosenberg,B., van Camp,L. and Krigas,T. (1965) Inhibition of cell division in *Escherichia coli* by electrolysis products from a platinum electrode. *Nature*, **205**, 698–699.
- O'Dwyer,P.J., Stevenson,J.P. and Johnson,S.W. (2000) Clinical pharmacokinetics and administration of established platinum drugs. *Drugs*, **59**, 19–27.
- Decatris,M.P., Sundar,S. and O'Byrne,K.J. (2004) Platinum-based chemotherapy in metastatic breast cancer: current status. *Cancer Treat. Rev.*, **30**, 53–81.
- Siddik,Z.H. (2003) Cisplatin: mode of cytotoxic action and molecular basis of resistance. *Oncogene*, **22**, 7265–7279.
- Timmer-Bosscha,H., Mulder,N.H. and de Vries,E.G. (1992) Modulation of *cis*-diamminedichloroplatinum(II) resistance: a review. *Br. J. Cancer.*, **60**, 227–238.
- Cornelison,T.L. and Reed,E. (1993) Nephrotoxicity and hydration management for cisplatin, carboplatin, and ormaplatin. *Gynecol. Oncol.*, **50**, 147–158.
- Cano,J.R., Catalan,B. and Jara,C. (1998) Neuronopathy due to cisplatin. *Rev. Neurol.*, **27**, 606–610.
- Smooenburg,G.F., De-Groot,J.C., Hamers,F.P. and Klis,S.F. (1999) Protection and spontaneous recovery from cisplatin-induced hearing loss. *Ann. NY Acad. Sci.*, **884**, 192–210.
- Kartalou M., Essigmann J.M. (2001), Mechanisms of resistance to cisplatin. *Mutat. Res.*, **478**, 23–43.
- Blommaert,F.A., van Dijk-Knijnenburg,H.C.M., Dijt,F.J., den Engelse,L., Baan,R.A., Berends,F. and Fichtinger-Schepman,A.M.J. (1995) Formation of DNA adducts by the anticancer drug carboplatin.

Different nucleotide sequence preferences *in vitro* and in cells. *Biochemistry*, **34**, 8474–8480.

- Johansson,A., Olsson,C., Nygren,O., Nilsson,M., Seiving,B. and Cavallin-Stahl,E. (1995) Pharmacokinetics and tissue distribution of cisplatin in nude mice: platinum levels and cisplatin-DNA adducts. *Cancer Chemother. Pharmacol.*, **37**, 23–31.
- Terheggen,P.M.A.B., Floot,B.G., Scherer,E., Begg,A.C., Fichtinger-Schepman,A.M.J. and den Engelse,L. (1987) Immunocytochemical detection of interaction products of *cis*-diamminedichloroplatinum(II) and *cis*-diammine (1,1-cyclobutanedicarboxylato) platinum(II) with DNA in rodent tissue sections. *Cancer Res.*, **47**, 6719–6725.
- Schellens,J.H.M., Ma,J., Planting,A.S., Th., van der Burg,M.E.L., van Meerten,E., de Boer-Dennert,M., Schmitz,P.I.M., Stoter,G. and Verweij,J. (1996) Relationship between the exposure to cisplatin, DNA-adduct formation in leucocytes and tumour response in patients with solid tumours. *Br. J. Cancer*, **73**, 1569–1575.
- Liedert,B., Materna,V., Schadendorf,D., Thomale,J. and Lage,H. (2003) Overexpression of cMOAT (MRP2/ABCC2) is associated with decreased formation of platinum-DANN adducts and decreased G2-arrest in melanoma cells resistant to cisplatin. *J. Invest. Dermatol.*, **121**, 172–176.
- Meijer,C., Timmer,A., de-Vries,E.G., Groten,J.P., Knol,A., Zwart,N., Dam,W.A., Sleijfer,D.T. and Mulder,N.H. (2000) Role of metallothionein in cisplatin sensitivity of germ-cell tumours. *Int. J. Cancer*, **85**, 777–781.
- Crul,M., Schellens,J.H.M., Beijnen,J.H. and Maliepaard,M. (1997) Cisplatin resistance and DNA repair. *Cancer Treat. Rev.*, **23**, 341–366.
- Chen,Z., Xu,X.S., Yang,J. and Wang,G. (2003) Defining the function of XPC protein in psoralen and cisplatin-mediated DANN repair and mutagenesis. *Carcinogenesis*, **24**, 1111–1121.
- Furuta,T., Ueda,T., Aune,G., Sarasin,A., Kraemer,K.H. and Pommier,Y. (2002) Transcription-coupled nucleotide excision repair as a determinant of cisplatin sensitivity of human cells. *Cancer Res.*, **62**, 4899–4902.
- McHugh,P.J., Spanswick,V.J. and Hartley,J.A. (2001) Repair of DNA interstrand crosslinks: molecular mechanisms and clinical relevance. *Lancet Oncol.*, **2**, 483–490.
- Fichtinger-Schepman,A.M.J., Lohman,P.H.M. and Reedijk,J. (1982) Detection and quantification of adducts formed upon interaction of diamminedichloroplatinum (II) with DNA, by anion-exchange chromatography after enzymatic degradation. *Nucleic Acids Res.*, **10**, 5345–5356.
- Reed,E., Parker,R.J., Gill,I., Bicher,A., Dabholkar,M., Vionnet,J.A., Bostick-Bruton,F., Tarone,R. and Muggia,F.M. (1993) Platinum-DNA adduct in leukocyte DNA of a cohort of 49 patients with 24 different types of malignancies. *Cancer Res.*, **53**, 3694–3699.
- Bonetti,A., Apostoli,P., Zaninelli,M., Pavanell,F., Colombatti,M., Cetto,G.L., Franceschi,T., Sperotto,L. and Leone,R. (1996) Inductively coupled plasma mass spectroscopy quantitation of platinum-DNA adducts in peripheral blood leukocytes of patients receiving cisplatin- or carboplatin-based chemotherapy. *Clin. Cancer Res.*, **2**, 1829–1835.
- Blommaert,F.A. and Saris,C.P. (1995) Detection of platinum-DNA adducts by ³²P-postlabelling. *Nucleic Acids Res.*, **23**, 126–132.
- Farah,N., Dresner,H.S., Searles,K.J., Winiarsky,R., Moosikasuwan,M., Cajigas,A., Hahm,S. and Steinberg,J.J. (2000) Cisplatin DNA adduct detection and depurination measured by ³²P DNA radiolabeling and two-dimensional thin-layer chromatography: a time and concentration study. *Cancer Invest.*, **18**, 314–326.
- Pluim,D., Maliepaard,M., van-Waardenburg,R.C., Beijnen,J.H. and Schellens,J.H. (1999) ³²P-postlabeling assay for the quantification of the major platinum-DNA adducts. *Anal. Biochem.*, **275**, 30–38.
- Fichtinger-Schepman,A.M.J., van Oosterom,A.T., Lohman,P.H.M. and Berends,F. (1987) *Cis*-diammine-dichloroplatinum (II)-induced DNA adducts in peripheral leukocytes from seven cancer patients: quantitative immunochemical detection of the adduct induction and removal after a single dose of *cis*-diamminedichloroplatinum (II). *Cancer Res.*, **47**, 3000–3004.
- Meijer,C., de Vries,E.G.E., Dam,W.A., Wilkinson,M.H.F., Hollema,H., Hoekstra,H.J. and Mulder,N.H. (1997) Immunocytochemical analysis of cisplatin-induced platinum-DNA adducts with double-fluorescence video microscopy. *Br. J. Cancer*, **76**, 290–298.
- Poirier,M.C., Lippard,S.J., Zwelling,L.A., Ushay,H.M., Kerrigan,D., Thill,C.C., Santella,R.M., Grunberger,D. and Yuspa,S.H. (1982) Antibodies elicited against *cis*-diamminedichloroplatinum (II)-modified DNA are specific for *cis*-diamminedichloroplatinum

- (II)—DNA adducts formed *in vivo* and *in vitro*. *Proc. Natl. Acad. Sci. USA*, **79**, 6443–6447.
29. Terheggen, P.M., Floot, B.G., Lempers, E.L., van Tellingen, O., Begg, A.C. and den Engelse, L. (1991) Antibodies against cisplatin-modified DNA and cisplatin-modified (di)nucleotides. *Cancer Chemother. Pharmacol.*, **28**, 185–191.
 30. Tilby, M.J., Johnson, C., Knox, R.J., Cordell, J., Roberts, J.J. and Dean, C.J. (1991) Sensitive detection of DNA modifications induced by cisplatin and carboplatin *in vitro* and *in vivo* using a monoclonal antibody. *Cancer Res.*, **51**, 123–129.
 31. Chao, C.C., Shieh, T.-C. and Huang, H. (1994) Use of a monoclonal antibody to detect DNA damage caused by the anticancer drug *cis*-diamminedichloroplatinum (II) *in vivo* and *in vitro*. *FEBS Lett.*, **354**, 103–109.
 32. Sundquist, W.I., Lippard, S.J. and Stollar, B.D. (1987) Monoclonal antibodies to DNA modified with *cis*- or *trans*-diamminedichloroplatinum (II). *Proc. Natl. Acad. Sci. USA*, **84**, 8225–8229.
 33. Meczes, E.L., Azim-Araghi, A., Ottley, C.J., Pearson, D.G. and Tilby, M.J. (2005) Specific adducts recognised by a monoclonal antibody against cisplatin-modified DNA. *Biochem. Pharmacol.*, **70**, 1717–1725.
 34. Reed, E., Sauerhoff, S. and Poirier, M.C. (1988) Quantitation of platinum-DNA binding after therapeutic levels of drug exposure: a novel use of graphite furnace spectrometry. *Atomic Spectroscopy*, **9**, 93–95.
 35. Eberle, G., Gluesenkamp, K.H., Drosdzio, W. and Rajewsky, M.F. (1990) Monoclonal antibodies for the specific detection of 3-alkyladenines in nucleic acids and body fluids. *Carcinogenesis*, **11**, 1753–1759.
 36. Barcellini, W., Borghi, M.O., Fain, C., Papa, N., Nicoletti, F. and Meroni, P.L. (1992) Enrichment of IgG Anti-DNA producing lymphoblastoid cell lines by antigen-coated immunomagnetic beads. *Clin. Immunol. Immunopathol.*, **65**, 39–44.
 37. Ossendorp, F.A., Bruning, P.F., Van den Brink, J.A.M. and De Boer, M. (1989) Efficient selection of high-affinity B cell hybridomas using antigen-coated magnetic beads. *J. Immunol. Methods*, **120**, 191–200.
 38. Collier, H.A. and Collier, B.S. (1983) Statistical analysis of repetitive subcloning by the limiting dilution technique with a view toward ensuring hybridoma monoclonality. *Hybridoma*, **2**, 91–96.
 39. Coulter, A.R., Cox, J.C., Harris, R.D. and Healey, K. (1989) An enzyme immunoassay for isotyping mouse monoclonal antibodies. *Med. Lab. Sci.*, **46**, 54–58.
 40. Hutchens, T.W. and Porath, J. (1986) Thiophilic adsorption of immunoglobulins—analysis of conditions optimal for selective immobilization and purification. *Anal. Biochem.*, **159**, 217–226.
 41. Fleming, J.O. and Pen, L.B. (1988) Measurement of the concentration of murine IgG monoclonal antibody in hybridoma supernatants and ascites in absolute units by sensitive and reliable enzyme-linked immunosorbent assays (ELISA). *J. Immunol. Methods*, **110**, 11–18.
 42. Seiler, F., Kirstein, U., Eberle, G., Hochleitner, K. and Rajewsky, M.F. (1993) Quantification of specific DNA *O*-alkylation products in individual cells by monoclonal antibodies and digital imaging of intensified nuclear fluorescence. *Carcinogenesis*, **14**, 1907–1913.
 43. Horton, J.K., Evans, O.M., Swann, K. and Swinburne, S. (1989) A new and rapid method for the selection and cloning of antigen-specific hybridomas with magnetic microspheres. *J. Immunol. Methods*, **124**, 225–230.
 44. Egeland, T., Hovdenes, A. and Lea, T. (1988) Positive selection of antigen-specific B lymphocytes by means of immunomagnetic particles. *Scand. J. Immunol.*, **27**, 439–444.
 45. Hebell, T. and Gotze, O. (1989) The isolation of B lymphocytes from human peripheral blood using antibodies coupled to paramagnetic particles and rosetting techniques. *J. Immunol. Methods*, **123**, 283–291.
 46. Hochleitner, K., Thomale, J., Nikitin, A. and Rajewsky, M.F. (1991) Monoclonal antibody-based, selective isolation of DNA fragments containing an alkylated base to be quantified in defined gene sequences. *Nucleic Acids Res.*, **19**, 4467–4472.
 47. Lau, A.H. (1999) Apoptosis induced by cisplatin nephrotoxic injury. *Kidney Int.*, **56**, 1295–1298.
 48. Kelland, L.R. (1994) The molecular basis of cisplatin sensitivity/resistance. *Eur. J. Cancer*, **30**, 725–727.
 49. Fichtinger-Schepman, A.M., van der Velde-Visser, S.D., van Dijk-Knijnenburg, H.C., van Oosterom, A.T., Baan, R.A. and Berends, F. (1990) Kinetics of the formation and removal of cisplatin-DNA adducts in blood cells and tumor tissue of cancer patients receiving chemotherapy: comparison with *in vitro* adduct formation. *Cancer Res.*, **50**, 7887–7894.
 50. Mustonen, R., Takala, M., Leppala, S. and Hemminki, K. (1989) Dose-dependence and stability of cisplatin binding to tissue DNA and blood proteins in rats. *Carcinogenesis*, **10**, 365–368.
 51. Knox, R.J., Friedlos, F., Lydall, D.A. and Roberts, J.J. (1986) Mechanism of cytotoxicity of anticancer platinum drugs: evidence that *cis*-diamminedichloroplatinum(II) and *cis*-diammine-(1,1-cyclobutane-dicarboxylato) platinum(II) differ only in the kinetics of their interaction with DNA. *Cancer Res.*, **46**, 1972–1979.
 52. Poirier, M.C., Reed, E., Shamkhani, H., Tarone, R.E. and Gupta-Burt, S. (1993) Platinum drug-DNA interactions in human tissues measured by cisplatin-DNA enzyme-linked immunosorbent assay and atomic absorbance spectroscopy. *Environ. Health Perspect.*, **99**, 149–154.